



## ALZHEIMER'S DISEASE

# A protein panel in cerebrospinal fluid for diagnostic and predictive assessment of Alzheimer's disease

Rafi Haque<sup>1,2</sup>, Caroline M. Watson<sup>1,2</sup>, Jiaqi Liu<sup>2</sup>, E. Kathleen Carter<sup>1,3</sup>, Duc M. Duong<sup>1,3</sup>, James J. Lah<sup>1,2</sup>, Aliza P. Wingo<sup>4,5</sup>, Blaine R. Roberts<sup>1,2,3</sup>, Erik C. B. Johnson<sup>1,2</sup>, Andrew J. Saykin<sup>6</sup>, Leslie M. Shaw<sup>7,8</sup>, Nicholas T. Seyfried<sup>1,2,3\*</sup>, Thomas S. Wingo<sup>1,2,9\*</sup>, Allan I. Levey<sup>1,2\*</sup>

Copyright © 2023 The Authors, some rights reserved; exclusive licensee American Association for the Advancement of Science. No claim to original U.S. Government Works

Alzheimer's disease (AD) is a neurodegenerative disease with heterogenous pathophysiological changes that develop years before the onset of clinical symptoms. These preclinical changes have generated considerable interest in identifying markers for the pathophysiological mechanisms linked to AD and AD-related disorders (ADRD). On the basis of our prior work integrating cerebrospinal fluid (CSF) and brain proteome networks, we developed a reliable and high-throughput mass spectrometry–selected reaction monitoring assay that targets 48 key proteins altered in CSF. To test the diagnostic utility of these proteins and compare them with existing AD biomarkers, CSF collected at baseline visits was assayed from 706 participants recruited from the Alzheimer's Disease Neuroimaging Initiative. We found that the targeted CSF panel of 48 proteins (CSF 48 panel) performed at least as well as existing AD CSF biomarkers (A $\beta$ <sub>42</sub>, tTau, and pTau<sub>181</sub>) for predicting clinical diagnosis, FDG PET, hippocampal volume, and measures of cognitive and dementia severity. In addition, for each of those outcomes, the CSF 48 panel plus the existing AD CSF biomarkers significantly improved diagnostic performance. Furthermore, the CSF 48 panel plus existing AD CSF biomarkers significantly improved predictions for changes in FDG PET, hippocampal volume, and measures of cognitive decline and dementia severity compared with either measure alone. A potential reason for these improvements is that the CSF 48 panel reflects a range of altered biology observed in AD/ADRD. In conclusion, we show that the CSF 48 panel complements existing AD CSF biomarkers to improve diagnosis and predict future cognitive decline and dementia severity.

## INTRODUCTION

Alzheimer's disease (AD) is a neurodegenerative disorder characterized by cognitive decline and dementia in the presence of amyloid- $\beta$  (A $\beta$ ) plaques and neurofibrillary tangles in the brain (1, 2). The presence of hallmark AD pathologies years before the onset of clinical symptoms has generated interest in markers to identify individuals at risk of progressive neurodegeneration (2–4). Imaging and cerebrospinal fluid (CSF) biomarkers that measure these hallmark AD pathologies include selective positron emission tomography (PET) ligands that quantify and localize both amyloid plaques and tau pathologies in the brain and biochemical assays that measure CSF A $\beta$ <sub>42</sub>, total tau (tTau), and phospho-tau<sub>181</sub> (pTau<sub>181</sub>) abundance. Moreover, fluorodeoxyglucose (FDG) PET and structural magnetic resonance imaging (MRI) are used as surrogate measures for neurodegeneration or synaptic loss in AD (5). On the basis of these findings, the AT(N) research framework has been proposed to classify AD based on the presence of amyloid plaques (A), neurofibrillary tangles (T), and neurodegeneration (N) (1).

Whereas current biomarkers have provided critical advances, expansion of biomarkers for AD and AD-related disorders (ADRDs) is important for several reasons. First, pathological complexity and heterogeneity is the rule, rather than the exception, with most AD dementia syndromes attributable to varying combinations of age-related pathologies, and amyloid plaque and neurofibrillary pathology are responsible for dementia in only ~40% of cases (6–8). The AT(N) framework also anticipates future development of additional biomarkers, ATX(N), with X representing other pathophysiological mechanisms beyond amyloid and tau (1, 5). Second, biomarkers of amyloid and tau do not accurately predict the extent of cognitive impairment, with cognitively impaired individuals often showing normal amyloid PET and CSF amyloid and 30 to 40% of cognitively unimpaired elderly individuals showing AD pathology (6–8). Third, biomarkers of the hallmark pathologies have limited prognostic ability for predicting disease progression. For these reasons, additional markers are needed for accurate tracking of a broader spectrum of pathophysiological mechanisms linked to AD.

Recent advances in large-scale molecular profiling technology have identified genetic, transcriptomic, and proteomic alterations in AD and led to the development of data-driven models of AD pathophysiology in postmortem human brain. In our prior work, we performed mass spectrometry (MS)–based proteomics of ~2000 brain tissues from the Accelerating Medicine Partnership for AD (AMP-AD) (9–15). To find suitable candidates for AD/ADRD markers, we recently used deep discovery–based proteomics on CSF samples to identify protein alterations in CSF that reflect brain AD/ADRD pathophysiology (16). On the basis of the CSF findings, we developed an accurate and reliable targeted MS assay

<sup>1</sup>Goizueta Alzheimer's Disease Research Center, Emory University School of Medicine, Atlanta, GA 30329, USA. <sup>2</sup>Department of Neurology, Emory University School of Medicine, Atlanta, GA 30329, USA. <sup>3</sup>Department of Biochemistry, Emory University School of Medicine, Atlanta, GA 30322, USA. <sup>4</sup>Division of Mental Health Atlanta VA Medical Center, Decatur, GA 30033, USA. <sup>5</sup>Department of Psychiatry, Emory University School of Medicine, Atlanta, GA 30329, USA. <sup>6</sup>Department of Radiology and Imaging Sciences, Indiana University School of Medicine, Indianapolis, IN 46204, USA. <sup>7</sup>Department of Pathology and Laboratory Medicine, University of Pennsylvania, Philadelphia, PA 19104, USA. <sup>8</sup>Center for Neurodegenerative Disease Research, University of Pennsylvania, Philadelphia, PA 19104, USA. <sup>9</sup>Department of Human Genetics, Emory University School of Medicine, Atlanta, GA 30322, USA.

\*Corresponding author. Email: alevey@emory.edu (A.I.L.); thomas.wingo@emory.edu (T.S.W.); nseyfri@emory.edu (N.T.S.)

using selected reaction monitoring (SRM) that measures a panel of 48 proteins with isotopically labeled peptide standards (17).

In this work, we tested the diagnostic and predictive utility of the CSF 48 panel in 706 individuals from the Alzheimer's Disease Neuroimaging Initiative (ADNI). Overall, the CSF 48 panel improved upon the ability of existing AT(N) biomarkers to monitor pathophysiological mechanisms strongly linked to AD and ADRD and improved prediction of disease progression, future cognitive decline, and hippocampal atrophy compared with existing AT(N) measures.

## RESULTS

All participants were recruited by ADNI study sites. Inclusion criteria in the current study were enrollment in either ADNI-2 or ADNI-GO and availability of baseline CSF. The dataset consisted of 706 eligible participants with an average age of  $72.2 \pm 7.3$  years and 48% female (Table 1). The baseline diagnoses in ADNI were made by the investigators on the basis of clinician judgment as described in the "Study design" section and blinded to biomarker status, with participants assigned as cognitively normal (31%), mild cognitive impairment (MCI, 53%), and AD (16%). Using previously established CSF thresholds for CSF  $A\beta_{42}$  of less than 980 pg/ml and pTau<sub>181</sub> greater than 21.8 pg/ml, samples were categorized into four groups: 36% A<sup>+</sup>T<sup>+</sup>, 18% A<sup>+</sup>T<sup>-</sup>, 16% A<sup>-</sup>T<sup>+</sup>, and 30% A<sup>-</sup>T<sup>-</sup> (Table 1).

### The CSF 48 panel estimates baseline clinical diagnosis

The CSF 48 panel targets 62 peptides to measure 48 proteins (Fig. 1A and table S1). Among the 48 proteins, 18 proteins were significantly increased in AD, whereas 4 were significantly decreased in AD [ $P < 0.05$ ,  $t$  test, false discovery rate (FDR)-corrected]. To understand the diagnostic utility of the CSF 48 panel compared with canonical AD CSF biomarkers  $A\beta_{42}$ , pTau<sub>181</sub>, and tTau, we used logistic regression to estimate differences between control and participants with AD for each CSF analyte (Fig. 1A and table S1). As expected,  $A\beta_{42}$ , pTau<sub>181</sub>, and tTau were the top single estimators of AD diagnosis, with areas under the curve (AUCs) of 0.84, 95% confidence interval (CI) [0.79, 0.8]; 0.82, 95% CI [0.77, 0.87]; and 0.80, 95% CI [0.75, 0.85], respectively. We found that the most abundant proteins and the strongest individual classifiers of AD in the CSF 48 panel were tyrosine 3-monooxygenase/tryptophan 5-monooxygenase activation protein zeta (YWHAZ) and beta (YWHAB), 14-3-3 proteins, with AUCs of 0.78. These proteins have been previously linked to AD and Creutzfeldt-Jakob disease in CSF (16, 18, 19) and are associated with many aspects of brain function including neural signaling, neuronal synaptogenesis, and neurodifferentiation (20). We also found an increased abundance and AUC of 0.70 for SPARC-related modular calcium binding 1 (SMOC1), a protein previously identified as a hub protein for the matrisomal/extracellular matrix-associated coexpression module, with the strongest associations to AD global pathology in postmortem brain (9, 10, 16). We also found modest increases in pyruvate kinase M1/2 (PKM1/2), malate dehydrogenase 1 (MDH1), enolase 1 (ENO1), and aldolase, fructose-bisphosphate A (ALDOA), proteins central to glycolysis, gluconeogenesis, and the citric acid cycle (table S1). The proteins most decreased in abundance in AD CSF were VGF nerve growth factor inducible (VGF) and secretogranin II (SCG2), neurosecretory granins involved in axonal or

synaptic vesicle transport, and neuronal pentraxin receptor (NPTXR) and neuronal pentraxin 2 (NPTX2), proteins involved in glutamatergic synaptic transmission and implicated in synaptic plasticity and memory (Fig. 1A and table S1). These data suggest that several proteins measured by the targeted approach could differentiate control and participants with AD nearly as well as the gold standard CSF biomarkers.

To understand the collective performance of the CSF 48 panel for predicting clinical AD dementia, we used penalized logistic regression to model the relationship between all proteins in the CSF 48 panel and AD clinical dementia. For comparison, the same model was fitted using the CSF 48 panel plus the canonical CSF biomarkers. For the CSF 48 panel, we estimated an AUC of 0.94, 95% CI [0.91, 0.97], whereas for canonical CSF biomarkers ( $A\beta_{42}$ , pTau<sub>181</sub>, and tTau), we estimated an AUC of 0.90, 95% CI [0.86, 0.94] (Fig. 1B). The AUC for the CSF 48 panel was significantly higher than that for the canonical CSF biomarkers alone ( $P < 0.01$ , permutation procedure; Fig. 1B). The combination of the CSF 48 panel and canonical CSF biomarkers had the highest AUC of 0.96, 95% CI [0.94, 0.99] (Fig. 1B) and significantly improved the AUC compared with existing CSF biomarkers ( $P < 0.001$ , permutation procedure; Fig. 1B). These results demonstrate the cumulative ability of the CSF 48 panel to accurately differentiate clinical AD dementia as well as or better than the gold standard markers of AD CSF biomarkers.

### The CSF 48 panel accurately estimates baseline FDG PET and hippocampal volume

Synaptic dysfunction and neuronal loss occur many years before overt clinical AD dementia and strongly correlate with dementia severity, motivating the development of biomarkers for assessing synaptic function in AD. FDG PET, a measure of the cerebral metabolic rate of glucose, and volumetric MRI, including hippocampal volume, have been used to reflect neurodegeneration—the "N" indicated in the AT(N) framework. To understand whether the proteins in the CSF 48 panel were associated with these changes in AD pathogenesis, we performed an association analysis, which included synaptic proteins dysregulated in AD brain, FDG PET, and MRI-derived hippocampal volume, separately. We found that 20 of the proteins in the CSF 48 panel associated with FDG PET and 15 proteins associated with both FDG PET and hippocampal volume ( $P < 0.01$ ,  $t$  test, FDR-corrected; fig. S1). The individual CSF analyte most strongly associated with FDG PET and hippocampal volume was CSF  $A\beta_{42}$ , with Pearson correlation coefficients ( $R$ ) of 0.43 and 0.35, respectively (fig. S1). We found that both FDG PET and hippocampal volume (HV) were positively associated with synaptic proteins decreased in AD, NPTX2 (FDG  $R = 0.32$ ; HV  $R = 0.28$ ), NPTXR (FDG  $R = 0.26$ ; HV  $R = 0.22$ ), VGF (FDG  $R = 0.24$ ; HV  $R = 0.13$ ), and SCG2 (FDG  $R = 0.2$ ; HV  $R = 0.14$ ). We also found that FDG PET and hippocampal volume were negatively associated with CSF pTau<sub>181</sub> (FDG  $R = -0.36$ ; HV  $R = -0.30$ ), CSF tTau (FDG  $R = -0.34$ ; HV  $R = -0.31$ ), YWHAZ (FDG  $R = -0.34$ ; HV  $R = -0.28$ ), YWHAB (FDG  $R = -0.30$ ; HV  $R = -0.26$ ), and, to a lesser extent, SMOC1 (FDG  $R = -0.23$ ; HV  $R = -0.14$ ; fig. S1). FDG PET and hippocampal volume showed even lower associations or were not associated with metabolic proteins PKM, ALDOA, calmodulin 2 (CALM2), and MDH1 ( $R < 0.15$ , fig. S1). Hemoglobin A/B (HBB and HBA) and albumin (ALB), blood-based proteins serving as negative internal controls in this study, did not vary

**Table 1. Demographic and clinical characteristics of study participants.**

	Control	MCI	Dementia	Overall
No. of participants	220	376	110	706
Age at enrollment				
Mean (SD)	73.1 (6.04)	71.1 (7.57)	74.0 (8.31)	72.2 (7.34)
Median [min, max]	72.7 [56.2, 85.9]	71.1 [55.0, 91.4]	74.8 [55.9, 90.3]	72.3 [55.0, 91.4]
Sex				
Female	123 (55.9%)	172 (45.7%)	45 (40.9%)	340 (48.2%)
Male	97 (44.1%)	204 (54.3%)	65 (59.1%)	366 (51.8%)
Clinical diagnosis				
Control	220 (100%)	0 (0%)	0 (0%)	220 (31.2%)
MCI	0 (0%)	376 (100%)	0 (0%)	376 (53.3%)
Dementia	0 (0%)	0 (0%)	110 (100%)	110 (15.6%)
AT(N) category				
A <sup>-</sup> T <sup>-</sup>	91 (41.4%)	116 (30.9%)	3 (2.7%)	210 (29.7%)
A <sup>-</sup> T <sup>+</sup>	53 (24.1%)	57 (15.2%)	6 (5.5%)	116 (16.4%)
A <sup>+</sup> T <sup>-</sup>	45 (20.5%)	69 (18.4%)	10 (9.1%)	124 (17.6%)
A <sup>+</sup> T <sup>+</sup>	31 (14.1%)	134 (35.6%)	91 (82.7%)	256 (36.3%)
APOE genotype				
e2-e2	0 (0%)	1 (0.3%)	0 (0%)	1 (0.1%)
e2-e3	26 (11.8%)	26 (6.9%)	2 (1.8%)	54 (7.6%)
e2-e4	3 (1.4%)	5 (1.3%)	1 (0.9%)	9 (1.3%)
e3-e3	131 (59.5%)	165 (43.9%)	34 (30.9%)	330 (46.7%)
e3-e4	53 (24.1%)	139 (37.0%)	48 (43.6%)	240 (34.0%)
e4-e4	7 (3.2%)	40 (10.6%)	25 (22.7%)	72 (10.2%)
MoCA				
Mean (SD)	25.9 (2.46)	23.4 (3.14)	17.3 (4.76)	23.2 (4.25)
Median [min, max]	26.0 [19.0, 30.0]	23.0 [14.0, 30.0]	18.5 [4.00, 25.0]	24.0 [4.00, 30.0]
Missing	4 (1.8%)	1 (0.3%)	4 (3.6%)	9 (1.3%)
CDR-SB				
Mean (SD)	0.0500 (0.158)	1.43 (0.853)	4.60 (1.73)	1.49 (1.74)
Median [min, max]	0 [0, 1.00]	1.25 [0.500, 4.50]	4.50 [1.00, 10.0]	1.00 [0, 10.0]

with FDG PET and hippocampal volume (fig. S1). Together, these data suggest that a reduction in FDG PET and hippocampal volume were linked to similar sets of proteins in CSF. The altered proteins indicate shared pathophysiologic changes, including reduced abundance of synaptic proteins and CSF A $\beta$ <sub>42</sub>, and increased abundance of the CSF tTau, pTau<sub>181</sub>, and two 14-3-3 proteins. In contrast, there were comparatively weak associations with metabolic proteins.

To assess the cumulative performance of the CSF 48 panel for estimating both FDG PET and hippocampal volume, we trained a penalized regression model for each of the following: the CSF 48 panel with and without canonical CSF biomarkers, CSF biomarkers alone, APOE genotype, and age. Canonical CSF biomarkers alone were able to predict FDG PET and hippocampal volume with an *R* of 0.49 and 0.41, respectively (FDG PET, *P* = 6.4 × 10<sup>-43</sup>, Fig. 1C; hippocampal volume, *P* = 2.1 × 10<sup>-27</sup>, Fig. 1D). However, we found that the highest correlation between the combination of the CSF 48 panel and canonical biomarkers could estimate FDG PET and hippocampal volume with an *R* of 0.60 and 0.55 (FDG PET, *P* = 1.2 × 10<sup>-68</sup>, Fig. 1D; hippocampal volume, *P* = 9.1 × 10<sup>-53</sup>, Fig. 1D) that significantly outperformed canonical CSF biomarkers alone (*P* < 0.001, permutation procedure). The CSF 48 panel could predict FDG PET and hippocampal volume with an *R* of 0.57 and an *R* of 0.54 (FDG PET, *P* = 4.1 × 10<sup>-62</sup>, Fig. 1C; hippocampal volume, *P* = 5.1 × 10<sup>-49</sup>, Fig. 1D) and outperformed age, APOE genotype, and canonical AD biomarkers (*P* < 0.001, permutation procedure). Because age was a significant estimator of hippocampal volume, we estimated hippocampal volume using age, CSF protein panel, and canonical biomarkers (*R* of 0.58, *P* = 1.0 × 10<sup>-58</sup>) and found significant improvement in performance compared with the CSF protein panel and canonical biomarkers alone (*P* < 0.001, permutation procedure).

### The CSF 48 panel estimates baseline cognitive function and clinical measures of AD dementia severity

Next, we examined how proteins in the CSF 48 panel were associated with cognitive measures and dementia symptom severity, which are generally not captured by canonical CSF biomarkers. We first performed an association analysis of proteins in the CSF 48 panel for the Montreal Cognitive Assessment (MoCA) and Clinical Dementia Rating scale Sum of Boxes (CDR-SB), separately. We found that 24 proteins associated with the MoCA score, and 19 proteins associated with CDR-SB (*P* < 0.01, *t* test, FDR-corrected; fig. S1). As expected, the plasma proteins HBB, HBA, and ALB did not vary with MoCA and CDR-SB (fig. S1). To understand the collective performance of the CSF 48 panel for predicting either baseline MoCA and CDR-SB, we trained a penalized regression model as described above for FDG PET and hippocampal volume. The canonical CSF biomarkers estimated MoCA and CDR-SB with an *R* of 0.45 and 0.47, respectively (MoCA, *P* = 2.4 × 10<sup>-36</sup>, Fig. 1E; CDR-SB, *P* = 1.9 × 10<sup>-39</sup>, Fig. 1F), highlighting the limitations of amyloid and tau biomarkers in predicting cognitive status and dementia severity. The CSF 48 panel estimated MoCA and CDR-SB with an *R* of 0.52 and 0.55 for MoCA and CDR-SB, respectively (MoCA, *P* = 6.6 × 10<sup>-50</sup>, Fig. 1E; CDR-SB, *P* = 3.8 × 10<sup>-56</sup>, Fig. 1F), which was an improvement from canonical CSF biomarkers alone (*P* < 0.01, permutation procedure), APOE genotype (*P* < 0.001, permutation procedure), and age (*P* < 0.001, permutation procedure). The combination of the CSF 48 panel and canonical CSF biomarkers estimated MoCA and CDR-SB with *R* values of

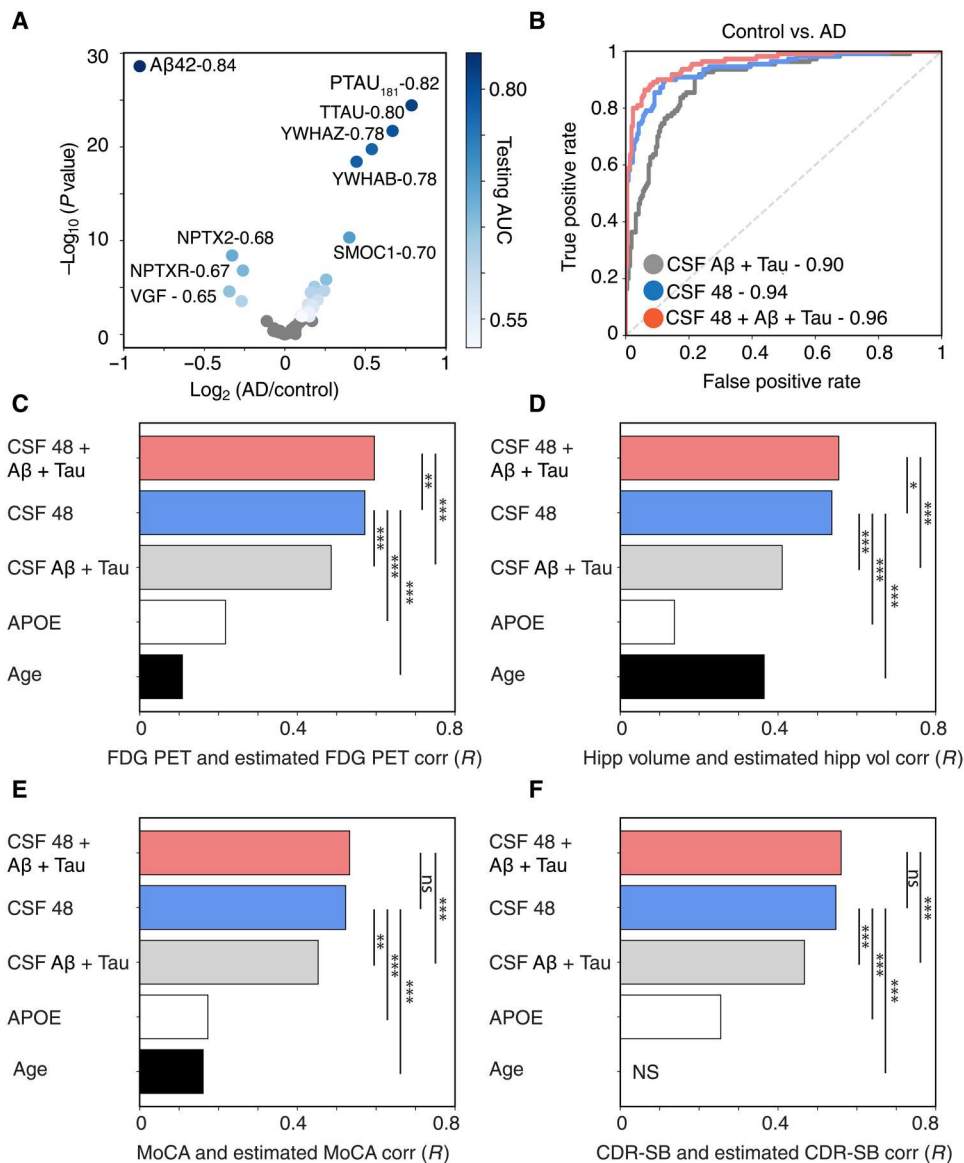


**Fig. 1. The CSF 48 panel estimates baseline cognitive FDG PET, hippocampal volume, cognitive status, and dementia severity in ADNI.** (A) Differential association analysis of all CSF analytes for clinical diagnosis of AD versus cognitively normal control. Analytes with FDR-adjusted significant association are shown in shades of blue that reflect their AUCs comparing controls with AD dementia. Nonsignificant proteins are shown in gray ( $P > 0.05$ , FDR-corrected). (B) The cumulative performance of canonical AD CSF biomarkers (“CSF A $\beta_{42}$  + Tau”), the CSF 48 panel (“CSF 48”), and the existing AD CSF biomarkers plus the CSF protein panel (“CSF 48 + CSF A $\beta_{42}$  + Tau”), estimated as the AUC for clinical diagnosis of AD versus cognitively normal control. Bar plots show the Pearson correlation coefficients between observed and predicted values of (C) FDG PET, (D) hippocampal volume (“Hipp Volume”), (E) Montreal Cognitive Assessment (MoCA), and (F) Clinical Dementia Rating scale Sum of Boxes (CDR-SB) for models using the following predictors: (i) the CSF protein panel plus existing AD CSF biomarkers plus (“CSF 48 + CSF A $\beta_{42}$  + Tau”), (ii) the CSF protein panel alone (“CSF 48”), (iii) canonical AD CSF biomarkers alone (“CSF A $\beta_{42}$  + Tau”), (iv) APOE E4 dose alone, or (v) age alone. \* $P < 0.05$ , \*\* $P < 0.01$ , and \*\*\* $P < 0.001$ . FDG-PET,  $n = 703$ ; hippocampal volume,  $n = 640$ ; MoCA,  $n = 694$ ; CDR-SB,  $n = 704$ . ns, not significant.

0.53 and 0.56 (MoCA,  $P = 4.1 \times 10^{-52}$ , Fig. 1E; CDR-SB,  $P = 2.2 \times 10^{-59}$ , Fig. 1F), outperforming the canonical CSF biomarkers alone ( $P < 0.001$ , permutation procedure). The performance of the CSF 48 panel for predicting either the MoCA or CDR-SB was the same as the performance of the CSF 48 panel plus canonical AD biomarkers ( $P > 0.05$ , permutation procedure; Fig. 1, E and F).

### The CSF 48 panel predicts changes in cognition, dementia severity, and hippocampal volume

Longitudinal studies like ADNI provide a powerful resource to study AD trajectories and develop prognostic biomarkers to predict rates of progression. Canonical biomarkers of amyloid and tau have limited prognostic ability, likely because additional molecular mechanisms contribute to the vulnerability and resilience of individuals that underlie variability in disease progression. We examined whether the proteins in the CSF 48 panel and

canonical CSF biomarkers could predict trajectories of cognition (MoCA), dementia severity (CDR-SB), and hippocampal volume. A minimum of at least three visits over a minimum of 3 years were required to estimate the trajectories for each participant (Table 2 and fig. S2). On average, controls showed a slower rate of cognitive decline compared with participants with MCI (MoCA,  $P = 8.51 \times 10^{-3}$ , *t* test; fig. S2) or AD (MoCA,  $P = 1.4 \times 10^{-25}$ , *t* test; fig. S2). Similarly, rates of decline on CDR-SB scores were significantly lower in controls than in participants with MCI (CDR-SB,  $P = 5.36 \times 10^{-6}$ , *t* test) and AD (CDR-SB,  $P = 2.2 \times 10^{-44}$ , *t* test). Testing for association between estimated trajectories and the individual proteins in the CSF 48 panel showed 24, 20, and 3 associated proteins with cognitive, dementia severity, and hippocampal changes, respectively ( $P < 0.01$ , *t* test, FDR-corrected, Fig. 2A). Among the individual CSF analytes, CSF pTau<sub>181</sub> was most strongly correlated with annual MoCA and CDR-SB change, *R* values of  $-0.49$  and  $0.42$ , followed by CSF tTau, YWHAZ, YWHAB, and CSF A $\beta_{42}$  (fig. S1). CSF A $\beta_{42}$  was most strongly correlated with annual hippocampal volume change with an *R* of  $0.36$ , followed by CSF pTau<sub>181</sub> ( $R = -0.33$ ), YWHAZ ( $R = -0.31$ ), CSF tTau ( $R = -0.30$ ), YWHAB ( $R = -0.27$ ), and SMOC1 ( $R = -0.22$ ) (Fig. 2A and fig. S1).

We next evaluated the collective prognostic potential of the CSF 48 panel compared with the canonical CSF biomarkers to predict each of the trajectories using a penalized multivariate linear regression model. First, annual MoCA change was estimated using both canonical CSF biomarkers ( $R = 0.52$ ,  $P = 1.98 \times 10^{-30}$ , Fig. 2, B and C) and the CSF 48 panel ( $R = 0.51$ ,  $P = 2.42 \times 10^{-28}$ , Fig. 2C), with no differences between the two measures ( $P > 0.05$ , permutation procedure). However, combining the CSF-targeted peptides with canonical CSF biomarkers significantly improved cognitive trajectory prediction ( $R = 0.62$ ,  $P = 9.12 \times 10^{-45}$ , Fig. 2C) compared with APOE genotype ( $P < 0.001$ , permutation procedure), canonical CSF biomarkers ( $P < 0.001$ , permutation procedure), or the CSF 48 panel alone ( $P < 0.001$ , permutation procedure). To predict rate of disease progression, annual CDR-SB change was also estimated using the canonical CSF biomarkers ( $R = 0.47$ ,  $P = 1.51 \times 10^{-24}$ , Fig. 2D) and the CSF 48 panel ( $R = 0.51$ ,  $P = 1.83 \times 10^{-29}$ , Fig. 2D). Combining the canonical biomarkers and the targeted panel improved the prediction of CDR-SB ( $R = 0.59$ ,  $P = 1.44 \times 10^{-41}$ , Fig. 2D) compared with the panel ( $P < 0.01$ , permutation procedure) and existing

biomarkers alone ( $P < 0.001$ , permutation procedure). For hippocampal volume trajectories, the model that combined the CSF 48 panel and canonical AD biomarkers resulted in the highest predicted correlation with observed change ( $R = 0.51$ ,  $P = 1.4 \times 10^{-16}$ , Fig. 2E) and was a significant improvement compared with CSF protein panel alone ( $R = 0.49$ ,  $P = 7.4 \times 10^{-15}$ ) or canonical CSF biomarkers ( $R = 0.39$ ,  $P = 1.2 \times 10^{-9}$ ) alone using permutation ( $P < 0.001$ ). Collectively, these results suggest that the CSF 48 panel, reflecting additional pathophysiologies beyond amyloid and tau, provides substantial value when combined with the canonical CSF biomarkers for predictions of cognition, dementia severity, and hippocampal changes compared with existing CSF biomarkers alone.

### The CSF 48 panel reveals distinct associations between existing CSF and PET biomarkers of AD

In vivo measurements of fibrillary amyloid in the brain using florbetapir (AV45) and other PET radioligands have emerged as important surrogate end points of AD pathophysiology (21) and are thought to reflect similar disease measures as CSF amyloid biomarkers because of their high concordance (1, 22, 23). Results of association testing between the CSF 48 panel and AV45 binding and the canonical CSF biomarkers A $\beta_{42}$ , p-tau, and t-tau are shown in Fig. 3A. AV45 binding was significantly associated with 25 CSF proteins (FDR  $P < 0.01$ , *t* test), whereas CSF A $\beta_{42}$  was associated with 21 proteins, with only 11 proteins showing an association with both CSF A $\beta_{42}$  and AV45 (Fig. 3A and fig. S1). CSF A $\beta_{42}$  was positively associated with VGF and SCG2, neurosecretory granins involved in synaptic vesicle transport, and NPTXR and NPTX2, pentraxin-associated proteins involved in glutamatergic synaptic transmission, indicating that low CSF A $\beta_{42}$  was associated with decreased abundance of synaptic proteins (Fig. 3A). Many of these synaptic proteins were not significantly associated with AV45 binding potential ( $P > 0.01$ , FDR-corrected, *t* test, Fig. 3A and fig. S1). Rather, AV45 binding was most strongly associated with SMOC1, a matrisomal protein that strongly correlated with amyloid plaques and global pathology in AD brain (9, 10), and YWHAZ and YWHAB (Fig. 3A). In contrast to CSF A $\beta_{42}$ , AV45 binding was also positively associated with a host of proteins associated with glucose metabolism, including PKM, PKM2, CALM2, ALDOA, MDH1, and lactate dehydrogenase B (LDHB; Fig. 3A and fig. S1). These results show discordance between the two amyloid biomarkers within the CSF peptide panel, with low CSF A $\beta_{42}$  most strongly linked to synaptic proteins decreased in AD and amyloid PET binding most strongly linked to matrisomal, 14-3-3 signaling, and metabolic proteins increased in AD.

In contrast to CSF A $\beta_{42}$  and PET amyloid biomarkers, CSF tTau and pTau<sub>181</sub> are thought to reflect related but distinct AD pathophysiology, with CSF tTau reflecting the intensity of synaptic loss and neurodegeneration and pTau<sub>181</sub> reflecting an AD-specific pathological state associated with paired helical filament tau formation (24). Association testing with the CSF 48 panel revealed significant positive associations with CSF tTau and CSF pTau<sub>181</sub> with the same 36 proteins ( $P < 0.01$ , FDR-corrected, *t* test, Fig. 3A). CSF tTau and pTau<sub>181</sub> were strongly associated with many proteins within our panel, reaching correlations of  $0.70$  to  $0.80$  (Fig. 3A). SMOC1, YWHAZ, and YWHAB proteins all showed strong, positive associations with CSF tTau and pTau<sub>181</sub>. Both tau markers also showed strong, positive associations with neuronal proteins ontologically linked to cellular energy storage and metabolism (Fig. 3A) (16).

**Table 2. Trajectories of cognition, dementia severity, and hippocampal volume in ADNI participants.**

	MoCA	CDR-SB	Hippocampal volume (mm <sup>3</sup> /year)
No. of participants	412	429	227
Age at enrollment	71.4 ± 7.0	71.6 ± 7.0	70.5 ± 7.2
Follow-up duration	5.79 ± 1.8	5.85 ± 1.8	4.08 ± 0.55
Number of visits	6.51 ± 1.5	6.58 ± 1.6	5.74 ± 0.95
Annual trajectory	-0.27 ± 0.90	0.30 ± 0.72	-127 ± 113.2

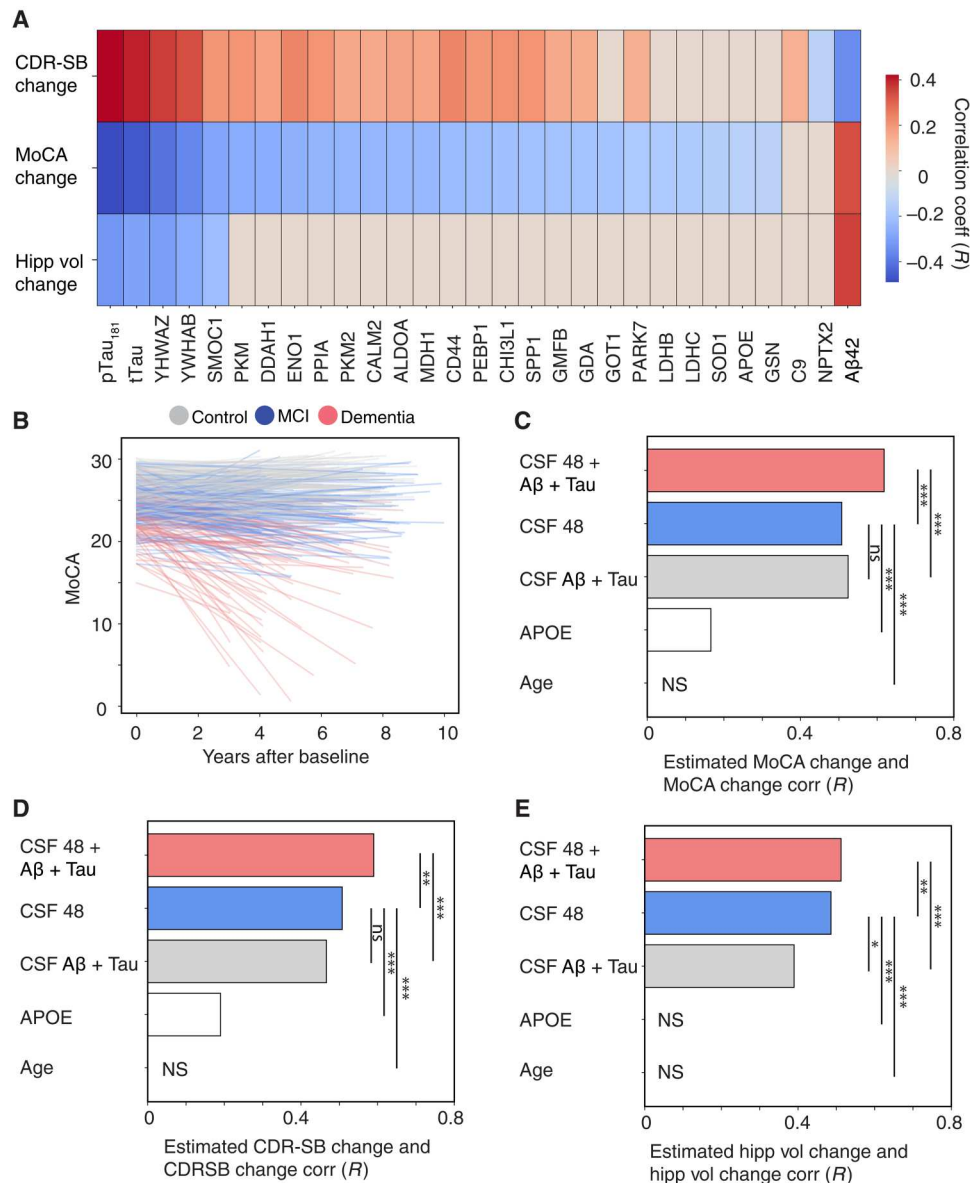


**Fig. 2. The CSF 48 panel predicts future change in cognition, dementia severity, and hippocampal volume.** (A) A heatmap of FDR-adjusted Pearson correlations is shown for CSF analytes and change in CDR-SB, MoCA, or hippocampal volume. The CSF peptides are labeled as their respective gene symbols, the strength and direction of correlation are shown by the red to blue scale, and nonsignificant correlations are shown as gray. (B) Line plot of individual estimates of MoCA decline over time. The color of each line reflects the baseline clinical diagnosis. Bar plots show the Pearson correlation coefficients between observed and predicted values. (C) MoCA, (D) CDR-SB, or (E) hippocampal volume for models using the following predictors: (i) the CSF protein panel plus existing AD CSF biomarkers plus ("CSF 48 + CSF Aβ<sub>42</sub> + Tau"), (ii) the CSF protein panel alone ("CSF 48"), (iii) canonical AD CSF biomarkers alone ("CSF Aβ<sub>42</sub> + Tau"), (iv) APOE E4 dose alone, or (v) age alone. \**P* < 0.05, \*\**P* < 0.01, \*\*\**P* < 0.001. MoCA, *N* = 412; CDR-SB, *n* = 429; hippocampal volume, *n* = 227.

PKM1/2, CALM2, ALDOA, and MDH1 are all proteins central to glycolysis, gluconeogenesis, and the citric acid cycle, indicating that the presence of tau pathology is tightly linked to altered glucose and energy metabolism in AD. CSF tau measures were also associated with aspartate aminotransferase GOT1, an important enzyme in amino acid metabolism, and guanine deaminase (GDA), an enzyme associated with purine metabolism and microtubule polymerization. These data suggest that elevated CSF tTau and pTau<sub>181</sub> may not only be linked to matrisomal dysfunction and impaired

14–3–3 signaling but also reflect widespread dysregulation across cellular energy and metabolism pathways.

### The CSF 48 panel accurately estimates existing CSF and PET biomarkers of AD

Following the approach for other studied outcomes, regularized linear regression was used to model the relationships between AV45 standard uptake value ratio (SUVR) with canonical CSF biomarkers, the CSF 48 panel, and a combination of canonical CSF biomarkers and the CSF 48 panel, separately. The performance of the

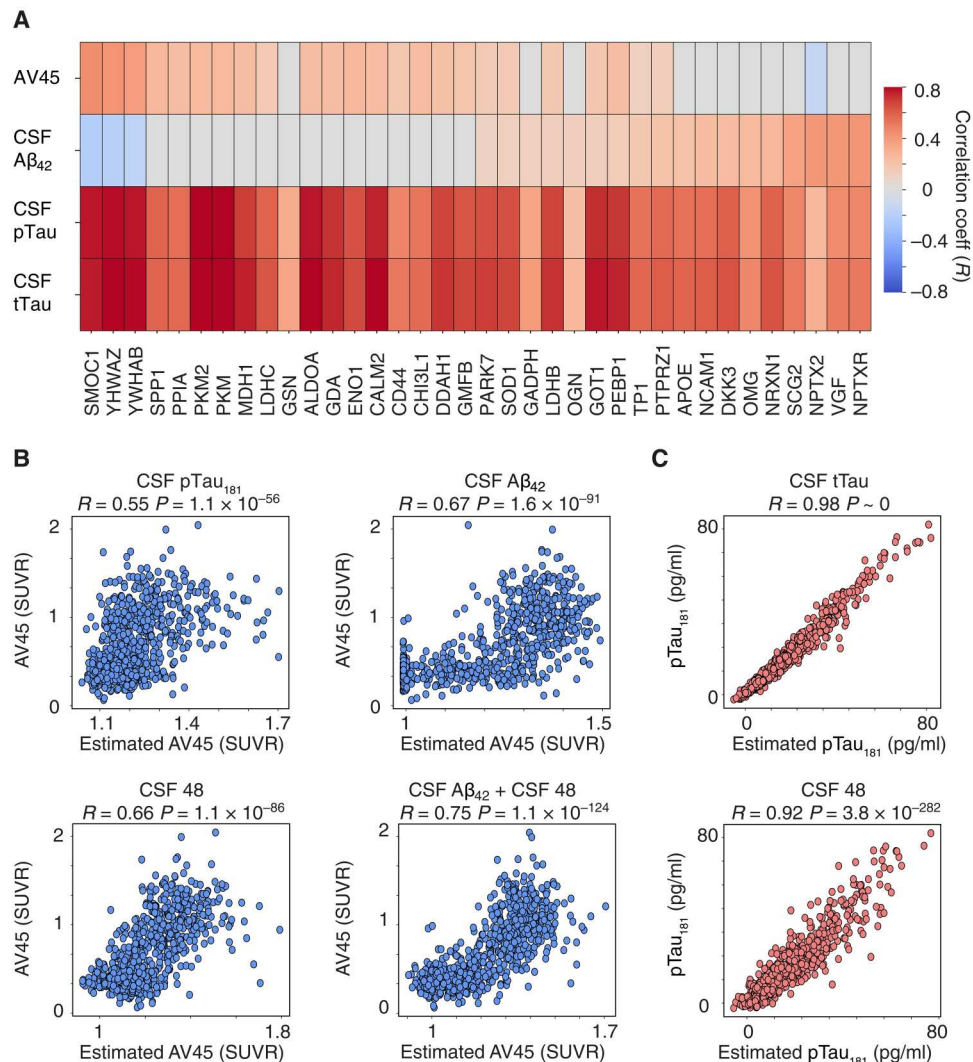


**Fig. 3. The CSF 48 panel estimates amyloid and tau biomarkers.** (A) Heatmaps of Pearson correlations are shown for CSF peptides that were significantly associated with one or more of the following outcomes after FDR adjustment: AV45 SUVR, CSF  $A\beta_{42}$ , CSF pTau<sub>181</sub>, and CSF tTau. The significant CSF peptides are labeled as their respective gene symbols, the strength and direction of the correlations are shown by the red to blue scale, and nonsignificant correlations are shown as gray (FDR,  $P < 0.01$ ,  $t$  test). (B) Scatterplot showing Pearson correlations between the observed and predicted estimate of AV45 SUVR using CSF pTau<sub>181</sub> (top left), CSF  $A\beta_{42}$  (top right), the CSF protein panel (“CSF 48,” bottom left), or the CSF protein panel plus CSF  $A\beta_{42}$  (“CSF  $A\beta_{42}$  + CSF 48,” bottom right). (C) Scatterplot showing Pearson correlations between the observed and predicted estimate of CSF pTau<sub>181</sub> using either CSF tTau (top) or the CSF protein panel (“CSF 48,” bottom) as predictors.

models was assessed by correlating the actual and estimated values for each predicted outcome. CSF pTau<sub>181</sub> and CSF  $A\beta_{42}$  estimated AV45 SUVR with an  $R$  of 0.55 ( $P = 1.1 \times 10^{-56}$ , Fig. 3B) and 0.67 ( $P = 1.6 \times 10^{-91}$ , Fig. 3B), respectively. The CSF 48 panel collectively estimated AV45 SUVR with an  $R$  of 0.66 ( $P = 1.1 \times 10^{-86}$ , Fig. 3B), and the CSF 48 panel combined with CSF  $A\beta_{42}$  improved the prediction to an  $R$  of 0.75 ( $P = 1.1 \times 10^{-124}$ , Fig. 3B), which reflected a significant improvement over the targeted CSF protein panel alone, CSF pTau<sub>181</sub>, or CSF  $A\beta_{42}$  ( $P < 0.001$ , permutation procedure). As expected, CSF tTau estimated CSF pTau<sub>181</sub> well at an  $R$  of 0.98 ( $P \sim 0$ , Fig. 3C), and the CSF 48 panel estimated CSF pTau<sub>181</sub> with an  $R$  of 0.92 ( $P = 3.78 \times 10^{-282}$ , Fig. 3C). These results show that the CSF 48 panel can accurately estimate AV45 binding, CSF  $A\beta_{42}$ , and CSF pTau<sub>181</sub>. Some of the discordance between the two amyloid biomarkers, AV45 SUVR and CSF  $A\beta_{42}$ , may be explained by different

synaptic, matrisomal, and metabolic pathophysiology reflected by the targeted CSF peptides.

### The CSF 48 panel accurately estimates baseline AT(N) status and improves estimation of cognitive decline

We next determined which proteins in the CSF 48 panel best classified AT(N) biomarker status and predicted changes in cognitive function or dementia. We stratified participants into those with and without evidence for both A and T pathologies ( $A^{+}T^{+}$  versus  $A^{-}T^{-}$ ) based on the canonical AD CSF biomarkers. An association analysis of proteins in the CSF 48 panel in  $A^{+}T^{+}$  versus  $A^{-}T^{-}$  individuals revealed that 34 proteins were significantly increased in  $A^{+}T^{+}$  compared with  $A^{-}T^{-}$  participants ( $P < 0.05$ ,  $t$  test, FDR-corrected, Fig. 4A), but no proteins were significantly decreased. SMOC1, YHWAZ, and YWHAB were the strongest differentiators

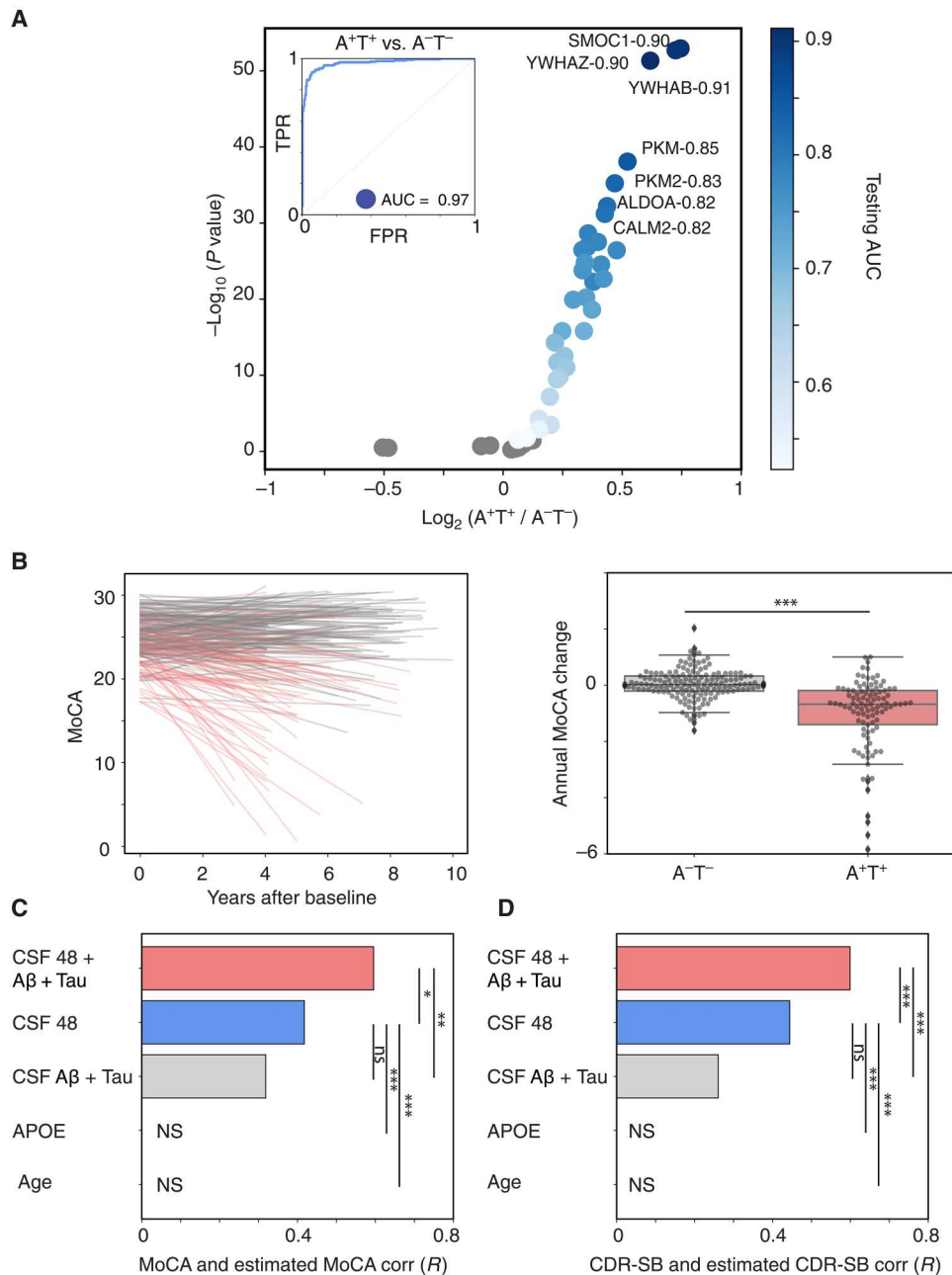


**Fig. 4. The CSF 48 panel predicts future change in cognition and dementia severity among patients with  $A^{+}T^{+}$  biomarker status.** (A) Analytes with FDR-adjusted significant association are shown in shades of blue that reflect their AUC comparing  $A^{+}T^{+}$  versus  $A^{-}T^{-}$  status. Nonsignificant proteins are shown in gray ( $P > 0.05$ , FDR-corrected). (B) (Left) A line plot of individual estimates of MoCA decline over time. The color of each line reflects the baseline A/T status. (Right) A box plot of the annual MoCA change for individuals with baseline  $A^{-}T^{-}$  and  $A^{+}T^{+}$ . Bar plots show the Pearson correlation coefficients between observed and predicted values of (C) MoCA or (D) CDR-SB for models using the following predictors: (i) the CSF protein panel plus existing AD CSF biomarkers plus ("CSF 48 + CSF  $A\beta_{42}$  + Tau"), (ii) the CSF protein panel alone ("CSF 48"), (iii) canonical AD CSF biomarkers alone ("CSF  $A\beta_{42}$  + Tau"), (iv) *APOE E4* dose alone, or (v) age alone. \* $P < 0.05$ , \*\* $P < 0.01$ , \*\*\* $P < 0.001$ . MoCA,  $n = 101$ ; CDR-SB,  $n = 113$ .

of  $A^{+}T^{+}$  and  $A^{-}T^{-}$  individuals, with AUCs ranging from 0.90 to 0.91 (Fig. 4A). The metabolic proteins PKM1/2, ALDOA, and CALM2 could also differentiate  $A^{+}T^{+}$  and  $A^{-}T^{-}$  individuals with high accuracy with AUCs of 0.82 to 0.85 (Fig. 4A and table S2). Synaptic proteins VGF, NPTXR, and SCG2 were much weaker differentiators of  $A^{+}T^{+}$  and  $A^{-}T^{-}$  individuals with AUCs ranging from

0.50 to 0.55 (Fig. 4A and table S2). The combination of the proteins in the CSF 48 panel could estimate the differences between  $A^{+}T^{+}$  and  $A^{-}T^{-}$  individuals with an AUC of 0.97, 95% CI [0.95, 0.98]. Because of the distinct proteomic profiles associating with CSF versus PET measures of amyloid shown earlier (Fig. 3), we also performed classification of amyloid PET-positive ( $AV45^{+}$ ) and

-negative individuals (AV45<sup>-</sup>) using an SUVR of 1.1. The CSF 48 panel could differentiate between AV45<sup>+</sup> and AV45<sup>-</sup> individuals with an AUC of 0.89, 95% CI [0.86, 0.92]. For comparison, we also classified individuals who were CSF A $\beta$ <sub>42</sub><sup>+</sup> (A<sup>+</sup>) and CSF A $\beta$ <sub>42</sub><sup>-</sup> (A<sup>-</sup>). The SRM proteome could separate these two populations with an AUC of 0.88, 95% CI [0.86, 0.91].

Whereas the AT(N) framework has been useful in identifying individuals at risk of cognitive decline, AD dementia syndromes are attributable to varying combinations of pathologies and pathophysiological processes, and therefore, substantial heterogeneity may exist even among A<sup>+</sup>T<sup>+</sup> individuals. Trajectories for cognitive decline and dementia severity were compared by baseline AT status. A<sup>-</sup>T<sup>-</sup> individuals showed a slower rate of cognitive decline compared with A<sup>+</sup>T<sup>+</sup> individuals (MoCA,  $P = 3.58 \times 10^{-17}$ , *t* test; CDR-SB,  $P = 5.32 \times 10^{-16}$ , *t* test; Fig. 4, B and C), which agrees with a prior study (25). For A<sup>+</sup>T<sup>+</sup> individuals, we trained a multivariate linear regression model to predict trajectories of cognition and dementia severity using the CSF 48 panel, the canonical CSF biomarkers, and the combination. The canonical CSF biomarkers alone modestly predicted disease trajectory (MoCA  $R = 0.32$ ,  $P = 1.18 \times 10^{-3}$ ; CDR-SB  $R = 0.26$ ,  $P = 5.33 \times 10^{-3}$ , Fig. 4, C and D). The CSF 48 panel somewhat better predicted these trajectories (MoCA  $R = 0.42$ ,  $P = 1.40 \times 10^{-5}$ ; CDR-SB  $R = 0.44$ ,  $P = 8.30 \times 10^{-7}$ , Fig. 4, C and D) but without a significant difference ( $P > 0.05$ , permutation procedure). However, the combination of the CSF 48 panel plus the canonical CSF biomarkers was significant in predicting both MoCA ( $R = 0.60$ ,  $P = 5.17 \times 10^{-11}$ ) and CDR-SB trajectory ( $R = 0.60$ ,  $P = 2.4 \times 10^{-12}$ , Fig. 4, C and D). The CSF 48 panel plus canonical CSF biomarkers showed a significant improvement in prediction over the canonical biomarkers ( $P < 0.001$ , permutation procedure). Overall, the CSF 48 proteome improves prediction of cognitive trajectory and dementia severity decline in at-risk individuals based on CSF amyloid and tau status.

## DISCUSSION

Here, we tested the diagnostic and prognostic characteristics of a targeted CSF protein panel measured on baseline CSF from 706 ADNI participants. This work builds on prior studies of postmortem brain proteomics that identified brain protein networks consistently altered in AD brain and protein alterations in CSF that reflect brain AD/ADRD pathophysiology (16). Here, we extended these findings using our recently developed SRM-MS assay with isotopically labeled peptide standards (17) to target and quantify 48 key proteins in baseline CSF samples from the ADNI study. The CSF 48 panel accurately predicted AD pathophysiology and disease as well as or better than the canonical CSF AD biomarkers, A $\beta$ <sub>42</sub>, tTau, and Tau<sub>181</sub>, with many individual proteins and the panel providing additional diagnostic and prognostic utility. The CSF 48 panel generally showed improved performance for predicting baseline AD imaging biomarkers (FDG PET, hippocampal volume, and AV45 SUVR) and measures of cognition and dementia severity (MoCA and CDR-SB). Moreover, when the CSF 48 panel was combined with the canonical AD CSF biomarkers, we observed improved predictive capabilities. The CSF 48 panel showed the ability to predict annual change in cognition (MoCA), dementia severity (CDR-SB), and neurodegeneration (hippocampal volume, FDG-PET) as well as or better than traditional AD CSF biomarkers and an additive improvement over existing AD CSF biomarkers

alone. As expected, the ability of the CSF 48 panel to predict progression was more pronounced among individuals whose CSF was consistent with a higher risk for having underlying AD pathophysiology. Together, the combined diagnostic and prognostic information of the CSF 48 panel, which measures additional pathophysiological processes beyond amyloid and tau, may improve identification of those at risk for AD and future decline.

The CSF 48 panel incorporated proteins across a range of dementia-related biological pathways and therefore was able to identify heterogeneity across the various AD markers. Because of their high concordance across individuals, CSF A $\beta$ <sub>42</sub> and amyloid PET have been generally thought to reflect the same underlying pathological state and are often used interchangeably as amyloid biomarkers (1, 22, 23). However, our findings revealed distinct proteomic signatures for CSF A $\beta$ <sub>42</sub> and amyloid PET. Low CSF A $\beta$ <sub>42</sub> most strongly linked to synaptic proteins decreased in AD, whereas amyloid PET binding was most strongly linked to increased abundance of matrisomal, 14-3-3 signaling, and metabolic proteins in AD. Thus, we advocate against using these biomarkers interchangeably.

A theme that emerged from this study was the strong, positive association between CSF tTau and pTau<sub>181</sub> with neuronal proteins ontologically linked to cellular energy storage and metabolism (16), with many metabolic proteins exhibiting correlation coefficients greater than 0.8. The correlation between CSF tau and glycolytic proteins has been observed in other studies (19, 26). Metabolic proteins could differentiate the presence of increased CSF tTau and pTau<sub>181</sub> with AUCs greater than 0.9. These metabolic proteins were not as strongly associated with CSF A $\beta$ <sub>42</sub>, AV45, hippocampal atrophy, and, unexpectedly, FDG PET. Unlike SMOC1, YWHAZ, and YWHAB, which were also strongly associated with CSF tTau and pTau<sub>181</sub>, the metabolic proteins were poor estimators of clinical diagnosis. Together, our data suggested that CSF tTau and pTau<sub>181</sub> are more tightly linked to cellular energy and metabolism compared with the other markers of AD. These findings also have potential biological implications that warrant future studies.

The CSF 48 panel was selected on the basis of integration of large-scale brain and CSF protein networks, providing an unbiased approach that also sheds light on the potential mechanisms underlying their roles in disease biology (10, 16). The divergence in CSF protein profiles associated with CSF A $\beta$ <sub>42</sub> and amyloid PET, respectively, points toward distinct pathophysiologicals linked to these two amyloid biomarkers. Unlike PET measures of fibrillar amyloid deposits in brain, low concentrations of CSF A $\beta$ <sub>42</sub> in AD were strongly associated with synaptic proteins that increased in CSF and decreased in brain (16). These changes begin early in the asymptomatic phases of disease (10, 16, 17) and, together with the metabolic changes noted above, may reflect synaptic plasticity, microglial pruning, and extrusion of synaptic material, as we and others have discussed previously (16, 27). We speculate that reductions in CSF A $\beta$ <sub>42</sub> thus reflect changes in synaptic biology rather than deposition into plaques in brain. In contrast, amyloid PET was strongly associated with increases in proteins linked to the matrisome and 14-3-3 signaling, including SMOC1, YWHAZ, and YWHAB. SMOC1 is one of the most differentially expressed proteins in AD brain and the hub protein in the matrisome module M42, which is highly correlated with AD neuropathology ( $r = 0.75$ ) and also contains A $\beta$ <sub>42</sub> and Apoe among its 32 protein members (9). Many of the proteins in this module bind heparin

and are histologically associated with A $\beta$  plaques (9, 28), potentially facilitating protein aggregation. As members of a synaptic module in brain (16), we speculate that the increased CSF abundance of 14-3-3 proteins reflect a neuritic response to A $\beta_{42}$  deposition. Thus, we suggest that these biomarkers are good biofluid proxies for A $\beta_{42}$  plaques in brain.

The CSF 48 panel also demonstrated specific proteins associated with FDG PET and hippocampal atrophy, currently considered biomarkers of neurodegeneration. Our results suggest that reductions in NPTX2 and NPTXR are associated with reduced FDG uptake and hippocampal volume loss. These results align with studies showing that NPTX2 and NPTXR down-regulation prevents homeostatic scaling of excitatory synapses, eventually leading to volume loss and cognitive dysfunction in AD (29, 30). Unexpectedly, FDG PET was more associated with decreased abundance of synaptic proteins rather than metabolic proteins, indicating that global measure of FDG uptake may reflect synaptic loss (or reduced synaptic activity) rather than brain glucose metabolism.

An advantage of this study was a large, well-characterized dataset consisting of a wide spectrum of individuals from ages 55 to 90 across the United States, who were not preselected based on discrete clinical categories or on the presence of amyloid and tau pathology. By using the well-characterized ADNI longitudinal dataset, several notable biological insights were identified. The CSF 48 panel significantly improved predictions for future declines in cognition, dementia severity, and hippocampal atrophy compared with the canonical AD CSF biomarkers and provided additional value when combined with existing CSF biomarkers for predicting these outcomes. Even among A<sup>+</sup>T<sup>+</sup> individuals, we found that the CSF 48 panel could nearly double the estimation of future cognitive decline and dementia risk. Future approaches to assess cognitive decline and dementia risk may therefore benefit from the incorporation of peptides such as those in our SRM panel representing multiple biological pathways.

Our study has limitations. The proteins in the CSF 48 panel were selected on the basis of differences in abundance between control and AD cases, with these populations defined using A $\beta_{42}$ , tTau, and pTau<sub>181</sub> thresholds (16). Thus, the selected proteins may be limited in their ability to find proteins relevant to clinical end points that are independent of amyloid and tau. In future studies, we plan to expand measured proteins that relate to clinical end points independent of AT(N). Another limitation is that the ADNI cohort is not representative of the diversity of the population, and the canonical AD biomarkers show important racial differences that pose challenges to clinical translation in real-world practice. Further investigation is needed in populations with greater disease heterogeneity and racial/ethnic diversity to understand the generalizability of these findings. Despite these limitations, the CSF 48 panel improves upon existing AT(N) biomarkers to predict many pathophysiological mechanisms linked to AD and ADRD brain; distinguish pathophysiological mechanisms based on their proteomic signature; and improve the prediction of disease progression and future changes in cognition, dementia severity, and hippocampal volume.

## MATERIALS AND METHODS

### Study design

The study was designed to identify whether a targeted CSF protein panel predicts future cognitive decline or dementia severity. To test the diagnostic utility of these proteins and compare them to existing AD biomarkers, CSF collected at baseline visits was assayed from 706 participants recruited from the ADNI. Samples were randomized and blinded for MS analyses.

ADNI is a longitudinal, observational study, with participant ages ranging from 55 to 90, designed to collect and validate biomarkers to predict progression to AD. ADNI was launched in 2003 as a public-private partnership with a primary goal of testing whether serial MRI, PET, other biological markers, and clinical and neuropsychological assessment can be combined to measure the progression of MCI and AD. Participant recruitment for ADNI is approved by the Institutional Review Board of each participating site. All ADNI participants undergo standardized diagnostic assessment that renders a clinical diagnosis of either control, MCI, or AD using standard research criteria (31). Control participants had no subjective memory complaints, tested normally on Logical Memory II of the Wechsler Memory Scale, and had a mini-mental state examination (MMSE) between 24 and 30 and a CDR of 0 with a memory box score of 0. MCI participants reported subjective memory concerns, exhibited abnormal memory function on Logical Memory II of the Wechsler Memory Scale, and had an MMSE between 24 and 30 and a CDR of 0.5 with a memory box score of at least 0.5. Participants with AD not only exhibited subjective memory concerns but also met the National Institute of Neurological and Communicative Disorders and Stroke (NINCDS) and the Alzheimer's Disease and Related Disorders Association (ARDA) criteria for probable AD. Participants with AD also showed abnormal memory function on the Logical Memory II subscale from the Wechsler Memory Scale and had an MMSE of 20 to 26 and a CDR of 0.5 or 0.1. Inclusion criteria for the current study were enrollment in ADNI2 or ADNI GO and an available baseline CSF sample. There was no overlap between the 706 ADNI participants in this study and the Emory ADRC cohort that was used to develop the targeted SRM assay (17). Individuals in this study had CSF assessments for A $\beta_{42}$ , tTau, and pTau<sub>181</sub> using the Elecsys immunoassay detection platform (Roche Diagnostics Corporation, Indianapolis, IN, USA) by ADNI investigators (32). We used ADNI-established thresholds of CSF A $\beta_{42}$  less than 980 pg/ml and pTau<sub>181</sub> greater than 21.8 pg/ml to categorize individuals as either positive or negative for the respective measure (A<sup>+</sup>T<sup>+</sup>, A<sup>-</sup>T<sup>+</sup>, A<sup>+</sup>T<sup>-</sup>, and A<sup>-</sup>T<sup>-</sup>) (32). We also separated individuals into AV45<sup>+</sup> and AV45<sup>-</sup> individuals using an SUVR of 1.1. To assess clinical outcomes, we used the MoCA scores and CDR-SB.

### Proteomic peptide measurement in CSF

The CSF protein panel measures 48 key proteins that were selected after evaluation of more than 200 tryptic peptides considered from integration of the brain and CSF proteome network analysis (16, 17). Technical details of the discovery and validation of the selected peptides are described in Watson *et al.* (17). The participants in Watson *et al.* were distinct from the current study. The CSF protein panel targets 62 peptides to measure the 48 proteins. To select the most informative peptides for the 48 proteins, a differential analysis of the baseline diagnosis of AD versus normal cognition

was performed. For proteins with more than one peptide measured, we selected the peptide that most strongly associated with AD diagnosis for all subsequent analyses (Fig. 1A and table S1). In brief, ADNI CSF aliquots were thawed and further aliquoted onto nine shallow-well plates. On each plate, two pooled references that mimic AD-like ( $A^{+}T^{+}$ ) and control-like ( $A^{-}T^{-}$ ) CSF were included for quality control. In parallel, 50  $\mu$ l of each sample CSF and quality control aliquot were reduced, alkylated, and denatured with tris-2(-carboxyethyl)-phosphine (5 mM), chloroacetamide (40 mM), and sodium deoxycholate (1%) in triethylammonium bicarbonate buffer (100 mM) at 95°C for 10 min, followed by a 10-min cool down at room temperature. CSF proteins were digested with Lys-C (Wako; 0.5  $\mu$ g; 1:100 enzyme-to-protein ratio) and trypsin (Promega; 5  $\mu$ g; 1:10 enzyme-to-protein ratio) overnight at 37°C. After digestion, heavy labeled standards (15  $\mu$ l per 50  $\mu$ l of CSF) were added to the peptide solutions, followed by acidification with a 1% trifluoroacetic acid (TFA) and 10% formic acid (FA) solution to a final concentration of 0.1% TFA and 1% FA (pH  $\leq$  2). Sample plates were placed on an orbital shaker at 300 rpm for at least 10 min to ensure proper mixing. Plates were centrifuged (4680 rpm) for 30 min to pellet the precipitated surfactant. Peptides were desalted with Oasis PRiME HLB 96-well, 30 mg of sorbent per well, solid-phase extraction (SPE) cleanup plates from Waters Corporation (Milford, MA) using a positive pressure system. Each SPE well was conditioned (500  $\mu$ l of methanol) and equilibrated twice (500  $\mu$ l of 0.1% TFA) before 500  $\mu$ l of 0.1% TFA and supernatant were added. Each well was washed twice (500  $\mu$ l of 0.1% TFA) and eluted twice (100  $\mu$ l of 50% acetonitrile/0.1% FA). All eluates were dried under centrifugal vacuum.

Each aliquot was reconstituted in 50  $\mu$ l of mobile phase A (0.1% FA). Resuspended peptides (20  $\mu$ l) were separated on an AdvanceBio Peptide Map Guard column (2.1 mm by 5 mm, 2.7  $\mu$ m, Agilent) connected to an AdvanceBio Peptide analytical column (2.1 mm by 150 mm, 2.7  $\mu$ m, Agilent) by a 1290 Infinity II system (Agilent) and monitored on a TSQ Altis Triple Quadrupole mass spectrometer (Thermo Fisher Scientific). The sample was developed over a 14-min gradient using mobile phase A (0.1% FA in water) and mobile phase B (B; 0.1% FA in acetonitrile) with a flow rate at 0.4 ml/min. The gradient was from 2 to 24% B over 12.1 min and then from 24 to 80% over 0.2 min and held at 80% B for 0.7 min. The mass spectrometer was set to acquire data in positive-ion mode using single reaction monitoring acquisition. Three transitions were acquired for each target analyte cycle time set to 0.8 s; Q1 resolution, 0.7 full width at half maximum (FWHM); Q2 resolution, 1.2 FWHM; and CID gas, 1.5 mtorr. Total area ratios for each peptide were calculated by summing the area for each light (3) and heavy (3) transition and dividing the light total area by the heavy total area using Skyline. There were nine total sample plates. Each plate was run independently with two quality control aliquots at the beginning, end, and after every 20 samples per plate.

## Statistical analysis

### Cognitive and volumetric trajectories

Cognitive trajectories were estimated by calculating the slope of the MoCA change from the baseline for each participant with a minimum of three visits and a minimum follow-up of 3 years. Cognitive trajectories 4 SD above or below the mean were removed given the inherent variability associated with cognitive trajectories calculated from small number of visits. Trajectories for CDR-SB and

hippocampal volume were calculated using the same approach for cognitive trajectory. The differences in cognitive, CDR-SB, and hippocampal volume trajectories by last cognitive diagnosis were compared using an unpaired, two-tailed, *t* test.

### Differential expression and correlational analysis

All differential expression analysis was performed using an unpaired, two-tailed *t* test for each outcome. Outcomes included AD clinical status and pairwise comparisons of individuals for published CSF  $A\beta_{42}$  and tTau threshold. Multiple hypothesis testing was accounted for using FDR-adjusted *P* value by the Benjamini-Hochberg method. We also used Pearson correlation to compare outcomes with individual peptide abundance. HBA, HBB, and ALB were not expected to vary with AD pathophysiology and, therefore, used as negative internal controls for differential expression and correlational analysis. The outcome variables of interest were CSF  $A\beta_{42}$ , CSF tTau, CSF pTau<sub>181</sub>, AV45, FDG PET, hippocampal volume, MoCA, CDR-SB, annual MoCA change, annual CDR-SB change, and hippocampal volume change. Similar to the analysis of trajectories, outcomes outside 4 SDs from the mean were removed.

### Classification and regression analysis

To test the predictive performance of each putative CSF protein for estimating clinical diagnosis, a logistic regression classifier (sklearn 0.24.2) was trained using a fivefold cross-validation to classify individuals as cognitively normal or AD. Performance was assessed using the area under the true-positive and false-positive rate from the receiver operating characteristic (ROC) curve. To determine the performance of demographic data, previously measured biomarkers, or the SRM CSF proteins generated by this study for estimating clinical diagnosis or dementia-related outcomes, we used multivariate logistic regression classifiers with elastic net regularization for dichotomous outcomes and multivariate linear regression with elastic net regularization for continuous outcomes. A fivefold cross-validation to select the best L1 ratio for regularization was implemented to generate classification or regression estimates for all participants. Performance was assessed using a single area under the ROC curve for classification models and correlating the true and estimated outcomes for regression models. A nonparametric bootstrap procedure was used to estimate CIs for AUC measurements. Other multivariate linear regressions with elastic net regularization were performed using a similar procedure.

We compared the predictive performance of the CSF peptides with existing biomarker or demographic data. A nonparametric permutation procedure was used to compare performance for logistic regression models or linear models trained using CSF peptides and existing biomarker or demographic data. Our null hypothesis was that across participants, the CSF peptides showed no difference in performance to existing biomarker or demographic data. We computed the true difference in performance for the CSF peptides and existing biomarker data. We then randomly permuted the estimation-generated CSF peptides and existing biomarkers for each participant and recomputed the difference in performance. Significance was established using 1000 permutations.

## Supplementary Materials

This PDF file includes:

Figs. S1 and S2

**Other Supplementary Material for this manuscript includes the following:**

Tables S1 and S2  
MDAR Revision Checklist

**REFERENCES AND NOTES**

- C. R. Jack Jr., D. A. Bennett, K. Blennow, M. C. Carrillo, B. Dunn, S. B. Haeberlein, D. M. Holtzman, W. Jagust, F. Jessen, J. Karlawish, E. Liu, J. L. Molinuevo, T. Montine, C. Phelps, K. P. Rankin, C. C. Rowe, P. Scheltens, E. Siemers, H. M. Snyder, R. Sperling, NIA-AA Research Framework: Toward a biological definition of Alzheimer's disease. *Alzheimers Dement.* **14**, 535–562 (2018).
- A. Serrano-Pozo, M. P. Frosch, E. Masliah, B. T. Hyman, Neuropathological alterations in Alzheimer disease. *Cold Spring Harb. Perspect. Med.* **1**, a006189 (2011).
- H. Braak, I. Alafuzoff, T. Arzberger, H. Kretschmar, K. Del Tredici, Staging of Alzheimer disease-associated neurofibrillary pathology using paraffin sections and immunocytochemistry. *Acta Neuropathol.* **112**, 389–404 (2006).
- H. Braak, D. R. Thal, E. Ghebremedhin, K. Del Tredici, Stages of the pathologic process in Alzheimer disease: Age categories from 1 to 100 years. *J. Neuropathol. Exp. Neurol.* **70**, 960–969 (2011).
- H. Hampel, J. Cummings, K. Blennow, P. Gao, C. R. Jack Jr., A. Vergallo, Developing the ATX(N) classification for use across the Alzheimer disease continuum. *Nat. Rev. Neurol.* **17**, 580–589 (2021).
- D. A. Bennett, J. A. Schneider, Z. Arvanitakis, J. F. Kelly, N. T. Aggarwal, R. C. Shah, R. S. Wilson, Neuropathology of older persons without cognitive impairment from two community-based studies. *Neurology* **66**, 1837–1844 (2006).
- D. S. Knopman, J. E. Parisi, A. Salviati, M. Floriach-Robert, B. F. Boeve, R. J. Ivnik, G. E. Smith, D. W. Dickson, K. A. Johnson, L. E. Petersen, W. C. McDonald, H. Braak, R. C. Petersen, Neuropathology of cognitively normal elderly. *J. Neuropathol. Exp. Neurol.* **62**, 1087–1095 (2003).
- J. L. Price, D. W. McKeel Jr., V. D. Buckles, C. M. Roe, C. Xiong, M. Grundman, L. A. Hansen, R. C. Petersen, J. E. Parisi, D. W. Dickson, C. D. Smith, D. G. Davis, F. A. Schmitt, W. R. Markesbery, J. Kaye, R. Kurlan, C. Hulette, B. F. Kurland, R. Higdon, W. Kukull, J. C. Morris, Neuropathology of nondemented aging: Presumptive evidence for preclinical Alzheimer disease. *Neurobiol. Aging* **30**, 1026–1036 (2009).
- E. C. B. Johnson, E. K. Carter, E. B. Dammer, D. M. Duong, E. S. Gerasimov, Y. Liu, J. Liu, R. Betarbet, L. Ping, L. Yin, G. E. Serrano, T. G. Beach, J. Peng, P. L. De Jager, V. Haroutunian, B. Zhang, C. Gaiteri, D. A. Bennett, M. Gearing, T. S. Wingo, A. P. Wingo, J. J. Lah, A. I. Levey, N. T. Seyfried, Large-scale deep multi-layer analysis of Alzheimer's disease brain reveals strong proteomic disease-related changes not observed at the RNA level. *Nat. Neurosci.* **25**, 213–225 (2022).
- E. C. B. Johnson, E. B. Dammer, D. M. Duong, L. Ping, M. Zhou, L. Yin, L. A. Higginbotham, A. Guajardo, B. White, J. C. Troncoso, M. Thambisetty, T. J. Montine, E. B. Lee, J. Q. Trojanowski, T. G. Beach, E. M. Reiman, V. Haroutunian, M. Wang, E. Schadt, B. Zhang, D. W. Dickson, N. Ertekin-Taner, T. E. Golde, V. A. Petyuk, P. L. De Jager, D. A. Bennett, T. S. Wingo, S. Rangaraju, I. Hajjar, J. M. Shulman, J. J. Lah, A. I. Levey, N. T. Seyfried, Large-scale proteomic analysis of Alzheimer's disease brain and cerebrospinal fluid reveals early changes in energy metabolism associated with microglia and astrocyte activation. *Nat. Med.* **26**, 769–780 (2020).
- S. Mostafavi, C. Gaiteri, S. E. Sullivan, C. C. White, S. Tasaki, J. Xu, M. Taga, H. U. Klein, E. Patrick, V. Komashko, C. McCabe, R. Smith, E. M. Bradshaw, D. E. Root, A. Regev, L. Yu, L. B. Chibnik, J. A. Schneider, T. L. Young-Pearse, D. A. Bennett, P. L. De Jager, A molecular network of the aging human brain provides insights into the pathology and cognitive decline of Alzheimer's disease. *Nat. Neurosci.* **21**, 811–819 (2018).
- R. A. Neff, M. Wang, S. Vatansver, L. Guo, C. Ming, Q. Wang, E. Wang, E. Horgusluoglu-Moloch, W. M. Song, A. Li, E. L. Castranio, J. Tcw, L. Ho, A. Goate, V. Fossati, S. Noggle, S. Gandy, M. E. Ehrlich, P. Katsel, E. Schadt, D. Cai, K. J. Brennan, V. Haroutunian, B. Zhang, Molecular subtyping of Alzheimer's disease using RNA sequencing data reveals novel mechanisms and targets. *Sci. Adv.* **7**, (2021).
- N. T. Seyfried, E. B. Dammer, V. Swarup, D. Nandakumar, D. M. Duong, L. Yin, Q. Deng, T. Nguyen, C. M. Hales, T. Wingo, J. Glass, M. Gearing, M. Thambisetty, J. C. Troncoso, D. H. Geschwind, J. J. Lah, A. I. Levey, A multi-network approach identifies protein-specific co-expression in asymptomatic and symptomatic Alzheimer's disease. *Cell Syst.* **4**, 60–72.e4 (2017).
- A. P. Wingo, E. B. Dammer, M. S. Breen, B. A. Logsdon, D. M. Duong, J. C. Troncoso, M. Thambisetty, T. G. Beach, G. E. Serrano, E. M. Reiman, R. J. Caselli, J. J. Lah, N. T. Seyfried, A. I. Levey, T. S. Wingo, Large-scale proteomic analysis of human brain identifies proteins associated with cognitive trajectory in advanced age. *Nat. Commun.* **10**, 1619 (2019).
- A. P. Wingo, W. Fan, D. M. Duong, E. S. Gerasimov, E. B. Dammer, Y. Liu, N. V. Harerimana, B. White, M. Thambisetty, J. C. Troncoso, N. Kim, J. A. Schneider, I. M. Hajjar, J. J. Lah, D. A. Bennett, N. T. Seyfried, A. I. Levey, T. S. Wingo, Shared proteomic effects of cerebral atherosclerosis and Alzheimer's disease on the human brain. *Nat. Neurosci.* **23**, 696–700 (2020).
- L. Higginbotham, L. Ping, E. B. Dammer, D. M. Duong, M. Zhou, M. Gearing, C. Hurst, J. D. Glass, S. A. Factor, E. C. B. Johnson, I. Hajjar, J. J. Lah, A. I. Levey, N. T. Seyfried, Integrated proteomics reveals brain-based cerebrospinal fluid biomarkers in asymptomatic and symptomatic Alzheimer's disease. *Sci. Adv.* **6**, eaaz9360 (2020).
- C. M. Watson, E. B. Dammer, L. Ping, D. M. Duong, E. Modeste, E. K. Carter, E. C. B. Johnson, A. I. Levey, J. J. Lah, B. R. Roberts, N. T. Seyfried, Quantitative mass spectrometry analysis of cerebrospinal fluid protein biomarkers in Alzheimer's disease. *Sci. Data* **10**, 261 (2023).
- M. Foote, Y. Zhou, 14-3-3 proteins in neurological disorders. *Int. J. Biochem. Mol. Biol.* **3**, 152–164 (2012).
- M. Zhou, R. U. Haque, E. B. Dammer, D. M. Duong, L. Ping, E. C. B. Johnson, J. J. Lah, A. I. Levey, N. T. Seyfried, Targeted mass spectrometry to quantify brain-derived cerebrospinal fluid biomarkers in Alzheimer's disease. *Clin. Proteomics* **17**, 19 (2020).
- B. Cornell, K. Toyo-Okita, 14-3-3 proteins in brain development: Neurogenesis, neuronal migration and neuromorphogenesis. *Front. Mol. Neurosci.* **10**, 318 (2017).
- V. L. Villemagne, V. Dore, S. C. Burnham, C. L. Masters, C. C. Rowe, Imaging tau and amyloid- $\beta$  proteinopathies in Alzheimer disease and other conditions. *Nat. Rev. Neurol.* **14**, 225–236 (2018).
- K. Blennow, N. Mattsson, M. Scholl, O. Hansson, H. Zetterberg, Amyloid biomarkers in Alzheimer's disease. *Trends Pharmacol. Sci.* **36**, 297–309 (2015).
- H. Zetterberg, B. B. Bendlin, Biomarkers for Alzheimer's disease—preparing for a new era of disease-modifying therapies. *Mol. Psychiatry* **26**, 296–308 (2021).
- B. Olsson, R. Lautner, U. Andreasson, A. Ohrfelt, E. Portelius, M. Bjeker, M. Holta, C. Rosen, C. Olsson, G. Strobel, E. Wu, K. Dakin, M. Petzold, K. Blennow, H. Zetterberg, CSF and blood biomarkers for the diagnosis of Alzheimer's disease: A systematic review and meta-analysis. *Lancet Neurol.* **15**, 673–684 (2016).
- C. R. Jack Jr., H. J. Wiste, T. M. Therneau, S. D. Weigand, D. S. Knopman, M. M. Mielke, V. J. Lowe, P. Vemuri, M. M. Machulda, C. G. Schwarz, J. L. Gunter, M. L. Senjem, J. Graff-Radford, D. T. Jones, R. O. Roberts, W. A. Rocca, R. C. Petersen, Associations of amyloid, tau, and neurodegeneration biomarker profiles with rates of memory decline among individuals without dementia. *JAMA* **321**, 2316–2325 (2019).
- J. M. Bader, P. E. Geyer, J. B. Muller, M. T. Strauss, M. Koch, F. Leybold, P. Koertvelyessy, D. Bittner, C. G. Schipke, E. I. Incesoy, O. Peters, N. Deigendesch, M. Simons, M. K. Jensen, H. Zetterberg, M. Mann, Proteome profiling in cerebrospinal fluid reveals novel biomarkers of Alzheimer's disease. *Mol. Syst. Biol.* **16**, e9356 (2020).
- P. J. Visser, L. M. Reus, J. Gobom, I. Jansen, E. Dicks, S. J. van der Lee, M. Tzolaki, F. R. J. Verhey, J. Popp, P. Martinez-Lage, R. Vandenberghe, A. Leo, J. L. Molinuevo, S. Engelborghs, Y. Freund-Levi, L. Froelich, K. Sleegers, V. Dobricic, S. Lovestone, J. Streffer, S. J. B. Vos, I. Bos; ADNI, A. B. Smit, K. Blennow, P. Scheltens, C. E. Teunissen, L. Bertram, H. Zetterberg, B. M. Tijms, Cerebrospinal fluid tau levels are associated with abnormal neuronal plasticity markers in Alzheimer's disease. *Mol. Neurodegener.* **17**, 27 (2022).
- B. Bai, X. Wang, Y. Li, P. C. Chen, K. Yu, K. K. Dey, J. M. Yarbro, X. Han, B. M. Lutz, S. Rao, Y. Jiao, J. M. Sifford, J. Han, M. Wang, H. Tan, T. I. Shaw, J. H. Cho, S. Zhou, H. Wang, M. Niu, A. Mancieri, K. A. Messler, X. Sun, Z. Wu, V. Pagala, A. A. High, W. Bi, H. Zhang, H. Chi, V. Haroutunian, B. Zhang, T. G. Beach, G. Yu, J. Peng, Deep multilayer brain proteomics identifies molecular networks in Alzheimer's disease progression. *Neuron* **106**, 700 (2020).
- K. A. Pelkey, E. Barksdale, M. T. Craig, X. Yuan, M. Sukumaran, G. A. Vargish, R. M. Mitchell, M. S. Wyeth, R. S. Petralia, R. Chittajallu, R. M. Karlsson, H. A. Cameron, Y. Murata, M. T. Colonnese, P. F. Worley, C. J. McBain, Pentraxins coordinate excitatory synapse maturation and circuit integration of parvalbumin interneurons. *Neuron* **85**, 1257–1329 (2015).
- M. F. Xiao, D. Xu, M. T. Craig, K. A. Pelkey, C. C. Chien, Y. Shi, J. Zhang, S. Resnick, O. Pletnikova, D. Salmon, J. Brewer, S. Edland, J. Wegiel, B. Tycko, A. Savonenko, R. H. Reeves, J. C. Troncoso, C. J. McBain, D. Galasko, P. F. Worley, NPTX2 and cognitive dysfunction in Alzheimer's Disease. *eLife* **6**, e23798 (2017).
- ADNI Procedures Manual, <https://adni.loni.usc.edu/wp-content/uploads/2008/07/adni2-procedures-manual.pdf>.
- L. M. Shaw, J. Q. Trojanowski, for the Alzheimer's Disease Neuroimaging Initiative, Methods Report, ADNI3: Batch analyses of Ab42, t-tau, and p-tau181 in ADNI1, GO, 2 CSF samples using the fully automated Roche Elecsys and cobas e immunoassay analyzer system, <https://adni.loni.usc.edu/wp-content/uploads/2018/04/PPT-set-102-PPSB-FTF-Boston-10-31-2017.pptx> [accessed 13 December 2022].

**Acknowledgments:** We are indebted to all individuals who have selflessly volunteered their time to participate in this study and to the ADNI teams responsible for recruitment, retention, and study participation. Data used in the preparation of this article were obtained from the Alzheimer's Disease Neuroimaging Initiative (ADNI) database ([adni.loni.usc.edu](http://adni.loni.usc.edu)). As such, the investigators within the ADNI contributed to the design and implementation of ADNI and/or provided data but did not participate in analysis or writing of this report. A complete listing of

ADNI investigators can be found at [http://adni.loni.usc.edu/wp-content/uploads/how\\_to\\_apply/ADNI\\_Acknowledgement\\_List.pdf](http://adni.loni.usc.edu/wp-content/uploads/how_to_apply/ADNI_Acknowledgement_List.pdf). **Funding:** This work was supported by the National Institute on Aging (AG066511 to A.I.L.; AG061357 to A.I.L. and N.T.S.; AG056533, AG072120, and AG075827 to A.P.W. and T.S.W.; AG070937 to J.J.L.; and RAG079170 to T.S.W.) and by the Foundation of NIH (AMP-AD 2.0 Proteomics to A.I.L. and N.T.S.). ADNI is supported by the National Institute on Aging (AG024904), the National Institute of Biomedical Imaging and Bioengineering, and the Department of Defense (W81XWH-12-2-0012) and through generous contributions from the following: AbbVie, Alzheimer's Association, Alzheimer's Drug Discovery Foundation, Araclon Biotech, BioClinica Inc., Biogen, Bristol-Myers Squibb Company, CereSpir Inc., Cogstate, Eisai Inc., Elan Pharmaceuticals Inc., Eli Lilly and Company, EuroImmun, F. Hoffmann–La Roche Ltd. and its affiliated company Genentech Inc., Fujirebio, GE Healthcare, IXICO Ltd., Janssen Alzheimer Immunotherapy Research & Development LLC, Johnson & Johnson Pharmaceutical Research & Development LLC, Lumosity, Lundbeck, Merck & Co. Inc., Meso Scale Diagnostics LLC, NeuroRx Research, Neurotrack Technologies, Novartis Pharmaceuticals Corporation, Pfizer Inc., Piramal Imaging, Servier, Takeda Pharmaceutical Company, Transition Therapeutics, and the Canadian Institutes of Health Research. **Author contributions:** J.J.L., N.T.S., T.S.W., and A.I.L. conceptualized and designed the study; R.H., J.L., E.K.C., A.P.W., and T.S.W. curated the data and performed analyses; C.M.W., D.M.D., and B.R.R. designed and performed assays; A.J.S. and L.M.S. provided samples and data; R.H. wrote the original draft, and N.T.S., T.S.W., and A.I.L. reviewed and edited the manuscript; J.J.L., N.T.S., T.S.W., and A.I.L. supervised the project; and all authors read and approved the manuscript. **Competing interests:** D.M.D., N.T.S., and A.I.L. are founders of EmTheraPro. R.H. is a consultant for EmTheraPro. T.S.W. is a cofounder of revXon. J.J.L. is a consultant for Roche Diagnostics. A.J.S. is on the Scientific Advisory Board for Bayer Oncology, Eisai; on the Dementia Advisory Board

for Siemens Medical Solutions USA Inc.; on the MESA Observational Study Monitoring Board for NIH NHLBI; and on Multiple ADRC and consortium External Advisory Board and the Editorial Office Support as Editor-in-Chief, Brain Imaging and Behavior for Springer-Nature Publishing. All other authors declare that they have no competing financial interests. **Data and materials availability:** The results published here are in whole or in part based on data obtained from the AMP-AD Knowledge Portal (<https://adknowledgeportal.synapse.org>). The AMP-AD Knowledge Portal is a platform for accessing data, analyses, and tools generated by the AMP-AD Target Discovery Program and other programs supported by the National Institute on Aging to enable open-science practices and accelerate translational learning. The data, analyses, and tools are shared early in the research cycle without a publication embargo on secondary use. Data are available for general research use according to the following requirements for data access and data attribution (<https://adknowledgeportal.synapse.org/#/DataAccess/Instructions>). Raw MS files and the SRM peptide data that were generated and analyzed as part of this study are available on Synapse (project SynID: 52288633). For up-to-date information on ADNI, see <https://adni-info.org>. All ADNI data are available on the ADNI website (<https://adni.loni.usc.edu/>). These SRM data are also available at <https://adni.loni.usc.edu/> as the "Emory University CSF Targeted MS" version 2022-10-19. Scripts for data analysis are also available at DOI 10.5281/zenodo.8188292. All data associated with this study are present in the paper or the Supplementary Materials.

Submitted 24 December 2022

Accepted 17 August 2023

Published 6 September 2023

10.1126/scitranslmed.adg4122

# Science Translational Medicine

## A protein panel in cerebrospinal fluid for diagnostic and predictive assessment of Alzheimer's disease

Rafi Haque, Caroline M. Watson, Jiaqi Liu, E. Kathleen Carter, Duc M. Duong, James J. Lah, Aliza P. Wingo, Blaine R. Roberts, Erik C. B. Johnson, Andrew J. Saykin, Leslie M. Shaw, Nicholas T. Seyfried, Thomas S. Wingo, and Allan I. Levey

*Sci. Transl. Med.* **15** (712), eadg4122. DOI: 10.1126/scitranslmed.adg4122

### View the article online

<https://www.science.org/doi/10.1126/scitranslmed.adg4122>

### Permissions

<https://www.science.org/help/reprints-and-permissions>

Use of this article is subject to the [Terms of service](#)

---

*Science Translational Medicine* (ISSN 1946-6242) is published by the American Association for the Advancement of Science. 1200 New York Avenue NW, Washington, DC 20005. The title *Science Translational Medicine* is a registered trademark of AAAS.

Copyright © 2023 The Authors, some rights reserved; exclusive licensee American Association for the Advancement of Science. No claim to original U.S. Government Works